A High-Capacity Organic Anode with Self-Assembled Morphological Transformation for Green Lithium-Ion Battery

Yan Wang[1], Wei Liu[1], Ruitian Guo[1], Qunting Qu[1], Honghe Zheng[1],*, Jingyu Zhang[1] & Yunhui Huang[2],*

[1] College of Energy & Collaborative Innovation Center of Suzhou Nano Science and Technology, Soochow University, Suzhou, Jiangsu, 215006, P. R. China

[2] School of Materials Science and Engineering, Tongji University, Shanghai, 201804, China

Corresponding Author

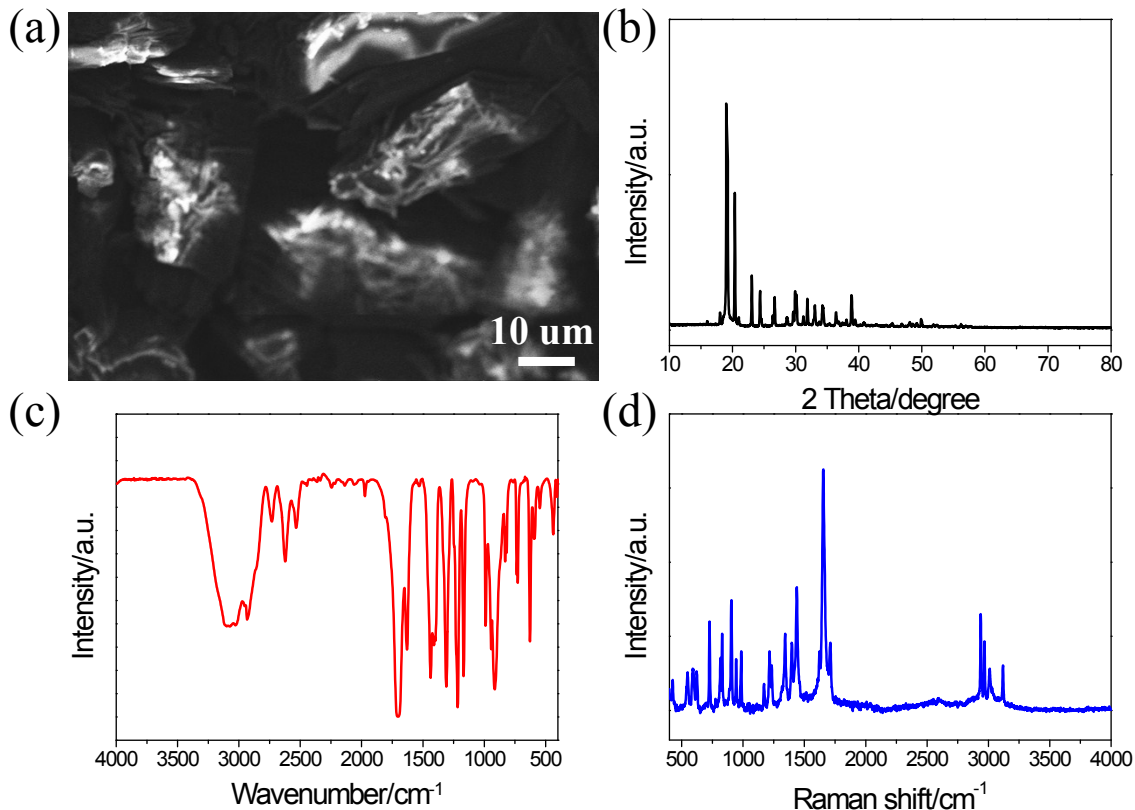E-mail: hhzheng@suda.edu.cn, huangyh@tongji.edu.cn

Figure S1 (a) SEM, (b) XRD (c) FTIR and (d) Raman spectrum of the IA powder.

Figure S2a shows the initial five charge/discharge curves of the AB anode (AB:CMC-SBR=4:1 wt%) without IA. The AB anode exhibits a first reversible capacity of 311 mAh g^{-1}, with a first coulombic efficiency of 56.3%. And the reversible capacity increased to 324 mAh g^{-1} in the second cycle, the coulombic efficiency increased to 88.4%. The capacity retains stable in the following cycles, and has a capacity of 321 mAh g^{-1} with a coulombic efficiency of 93.4% in the fifth cycle. Figure S2b shows the rate capability of the AB anode. At the current density of 300 and 600 mA g^{-1}, the AB anode exhibits a specific capacity of 327 and 325 mAh g^{-1}, respectively. At the current density of 1.5, 3, 6 and 15 A g^{-1}, the AB anode exhibits a specific capacity of 295, 274, 259 and 253 mAh g^{-1}, respectively.
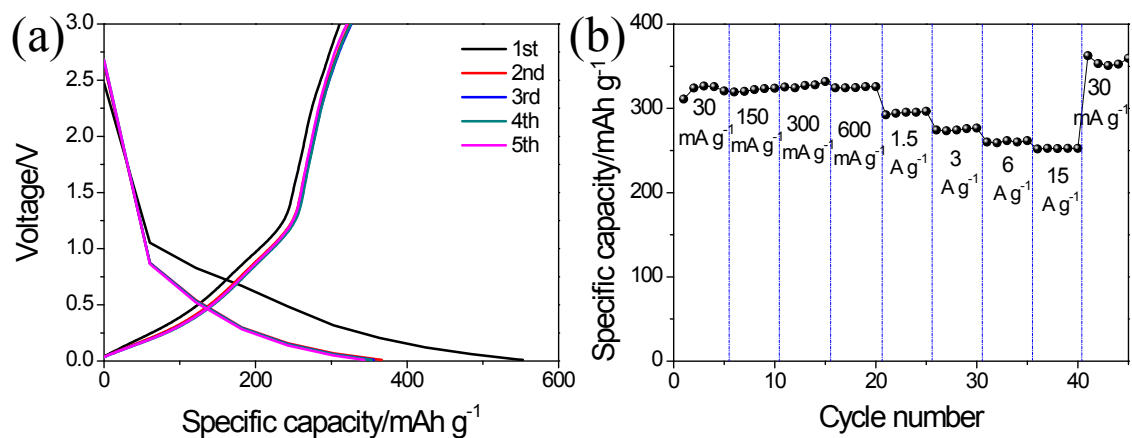
Figure S2 (a) The initial five charge/discharge curves at 30 mA g^{-1} and (b) the rate capability of the AB anode (AB:CMC-SBR=4:1 wt%) at various current densities.

Figure S3 shows the effect of the electrode thickness on the electrochemical performance of the IA anode. All the electrode thicknesses are final thickness with copper foil. Figure S3a shows an obvious decrease of the reversible capacity at the first cycle with increasing electrode thickness. As shown in Figure S3b, for the electrode with thicknesses of 30, 40, 50, 60 and 70 um (corresponding to the active loading of 0.40, 0.45, 0.51, 0.72 and 0.95 mg cm^{-2}), the reversible capacity in the first cycle is obtained to be 1270, 995, 880, 705 and 541 mAh g^{-1}, respectively. The corresponding coulombic efficiency is 66.2, 63.8, 61.6, 58.1 and 54.9%, respectively.
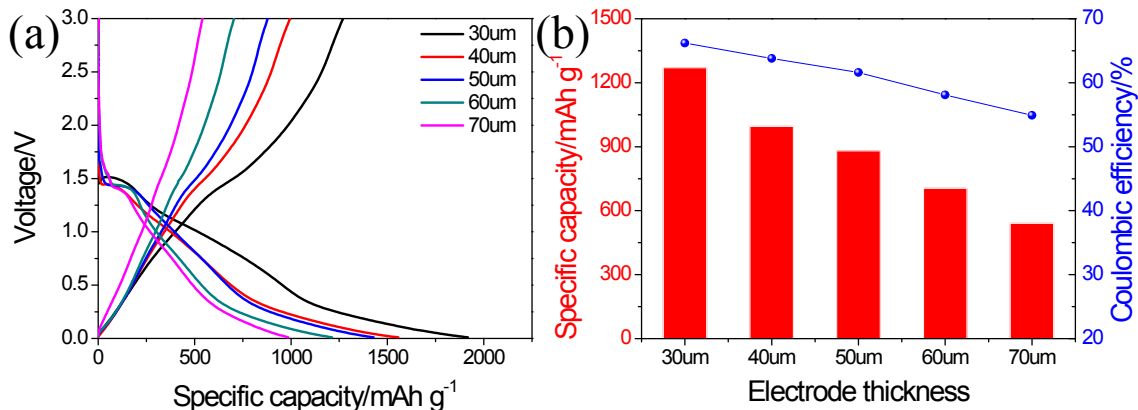
Figure S3 (a) The first charge/discharge profiles of the IA electrodes (IA:AB:CMC-SBR=5:4:1 wt%) with different thicknesses at the current density of 30 mA g^{-1} and (b) the corresponding reversible capacity and the first coulombic efficiency at different electrode thicknesses.

The first charge/discharge curves of the IA anodes with different compositions are displayed in Figure S4a. As shown in Figure S4a, the IA electrode shows an obvious decrease of the electrode polarization with increasing AB content. And the plateau started at *ca.* 1.5 V gradually shorted with the decrease of the AB content, this mainly because of the lack of AB leads to incomplete "activation" of IA, which corresponding to the process of the irreversible replacement of the hydrogen on the carboxyl group of IA with Li ions. Figure S4b compares the first reversible specific capacity and the coulombic efficiency of the IA anodes with different compositions. For the electrode with 40 wt% AB, the reversible capacity is obtained to be 1270 mAh g^{-1} and the first coulombic efficiency is 66.2%. By contrast, a reversible capacity of 811 mAh g^{-1} is obtained for the electrode with 30 wt% AB with the first coulombic efficiency of 52.4%. With 20 wt% AB, a reversible capacity of 576 mAh g^{-1} and the first coulombic efficiency of 47.0% are obtained. With 10 wt% AB, only 526 mAh g^{-1} of the reversible capacity and 36.6% of the first coulombic efficiency are obtained.
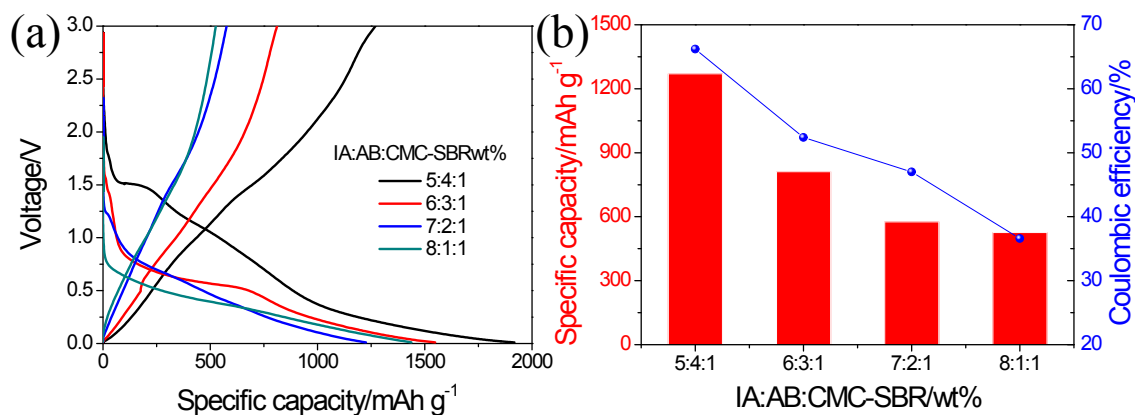
Figure S4 (a) The first charge/discharge profiles of the IA anodes with different compositions (IA:AB:CMC-SBR=9-x:x:1, x=4, 3, 2, 1 wt%) at the current density of 30 mA g^{-1} and (b) the corresponding reversible capacity and the coulombic efficiency.

Figure S5 shows the initial five charge/discharge profiles of the IA electrode at a current density of 30 mA g^{-1} between 0.01 and 3 V. The first charge and discharge capacities are obtained to be 1149 and 563 mAh g^{-1}, respectively; corresponding to the first CE of 49.0%. In the second cycle, the discharge capacity decreases to 506 mAh g^{-1} with a CE of 91.2%. In the third cycle, the discharge capacity reduces to 478 mAh g^{-1} and the CE is 92.5%.
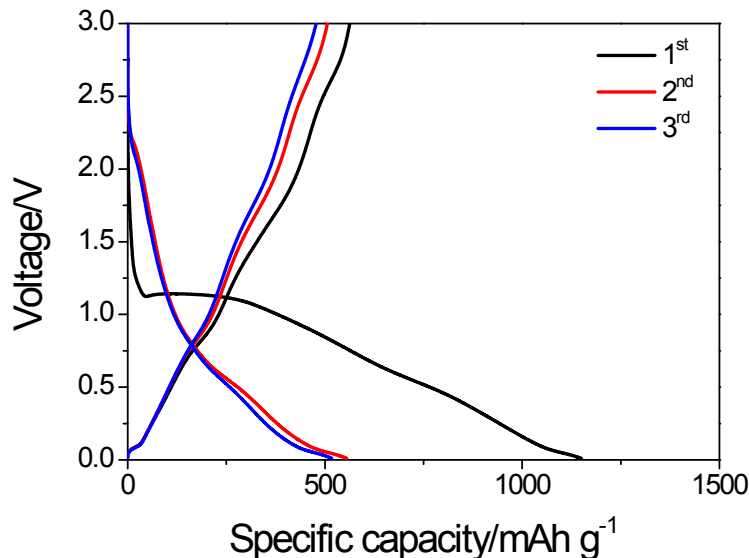
Figure S5 The initial three charge/discharge profiles of the IA anode (IA:AB:CMC-SBR=5:4:1 wt%) for sodium ion batteries at the current density of 30 mA g^{-1} between 0.01 and 3 V.

Figure S6 shows the electrochemical performances of the SP anode (SP:CMC-SBR=4:1 wt%) and IA anode (IA:SP:CMC-SBR=5:4:1 wt%). As shown in Figure S6a, the SP anode exhibits a first reversible capacity of 288 mAh g^{-1}, with a first coulombic efficiency of 59.7%. And the reversible capacity retains stable during the following cycles. Figure S6b shows the rate capability of the SP anode. At the current density of 1.5, 3, 6 and 15 A g^{-1}, the AB anode exhibits a specific capacity of 261, 237, 223 and 220 mAh g^{-1}, respectively. Figure S6c shows the initial five charge/discharge curves of the IA anode with SP as conductive agent. The first reversible capacity of the IA anode is 1099 mAh g^{-1}, with a first coulombic efficiency of 65.3%. In the subsequent cycles, the reversible capacity slightly increases with cycle number and reaches to 1358 mAh g^{-1} after five electrochemical cycles. Figure S6d shows the rate capability of the IA anode. At the discharge current density of 1.5, 3, 6 and 15 A g^{-1}, the specific capacity is obtained to be 1474, 1075, 920 and 683 mAh g^{-1}, respectively.
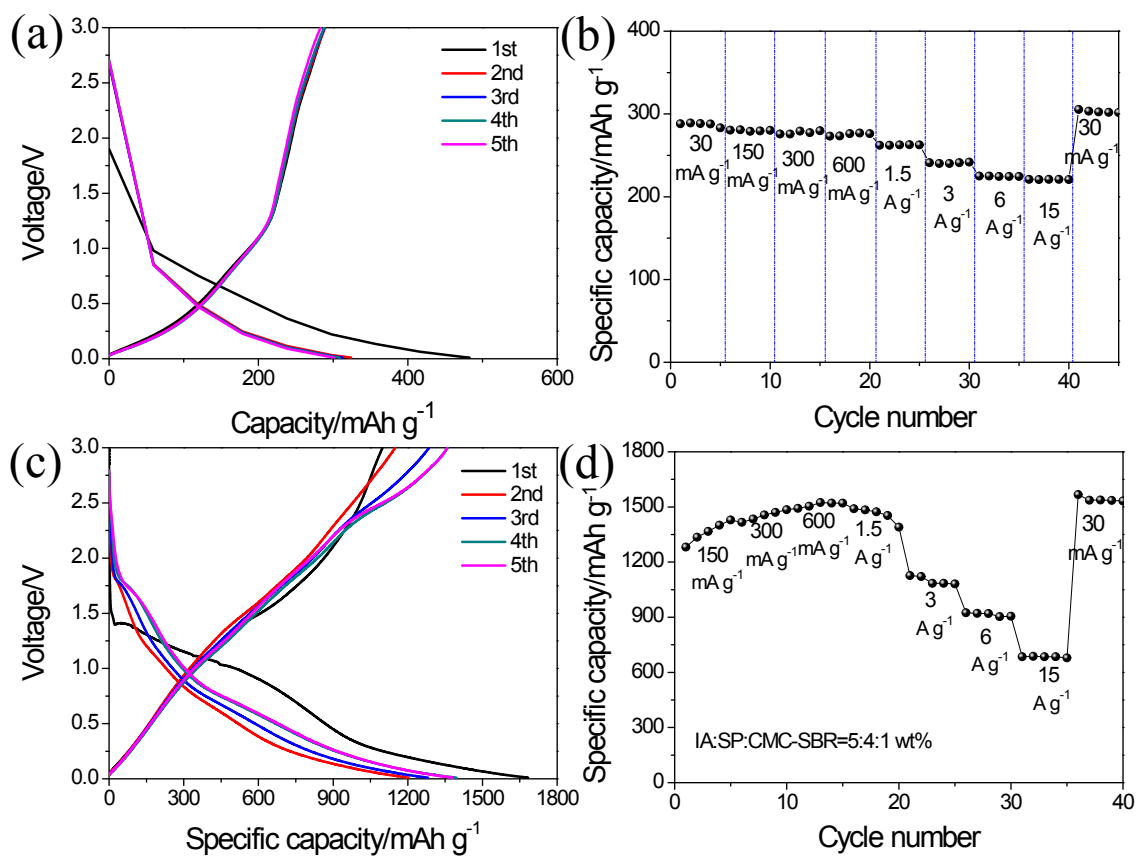
Figure S6 (a) The initial five charge/discharge curves at 30 mA g^{-1} and (b) the rate capability of the SP anode (SP:CMC-SBR=4:1 wt%) at various current densities; (c) The initial five charge/discharge curves at 30 mA g^{-1} and (d) the rate capability of the IA anode (IA:SP:CMC-SBR=5:4:1 wt%) at various current densities.

Figure S7 compares the electronic conductivities of the IA powder, AB powder and IA anode laminate (IA:AB:CMC-SBR=5:4:1 wt%). The electronic conductivity of the IA powder is too low to test, this is a common phenomenon for organic materials. The electronic conductivity of AB powder and IA anode laminate (IA:AB:CMC-SBR=5:4:1 wt%) is 0.36 and 0.07 S cm^{-1}, respectively. This result verified that adding conductive carbon is an effective and necessary method to ensure the electronic conductivity of organic electrodes.
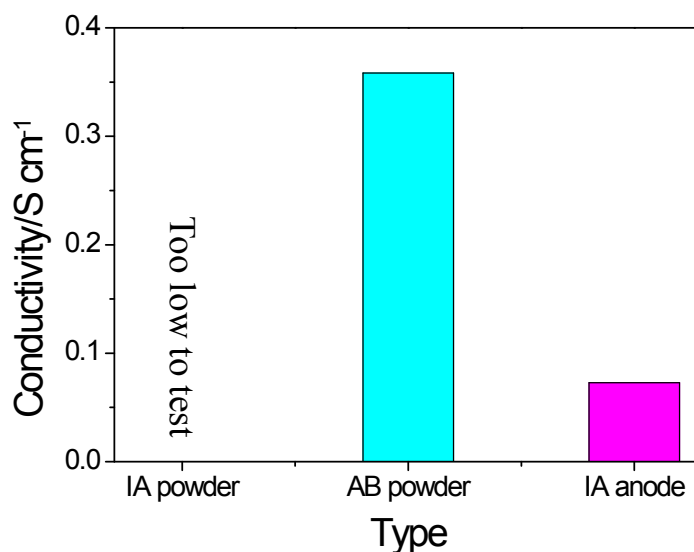

Figure S7 Electronic conductivities of the IA powder, AB powder and IA anode laminate (IA:AB:CMC-SBR=5:4:1 wt%).

To test the solubility of the IA in the electrolyte (1 mol L^{-1} LiPF$_6$ dissolved in a mixed solvent of ethylene carbonate/diethylene carbonate/dimethyl carbonate, v/v/v=1:1:1), we added 1 g IA powder into 2 g electrolyte (see Figure S8). After a little time, the stratification can be clearly observed (see photo A). Photo B is the sample A after sonicating for 30 minutes, it's clearly to see IA powder is not dissolved in the electrolyte. And after seven days' standing of sample B, IA powder is still not dissolved in the electrolyte and the stratification phenomenon is very obvious

(see photo C). All these results indicate the IA powder is not soluble in the electrolyte, this is consistent with the good cycling performance of the IA anode.
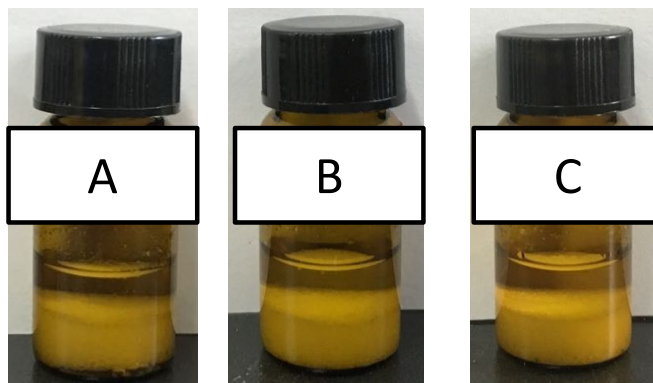

Figure S8. The photo of the 1 g IA powder added into 2 g electrolyte after (A) a little time, (B) sonicating for 30 minutes and (C) seven days' standing.
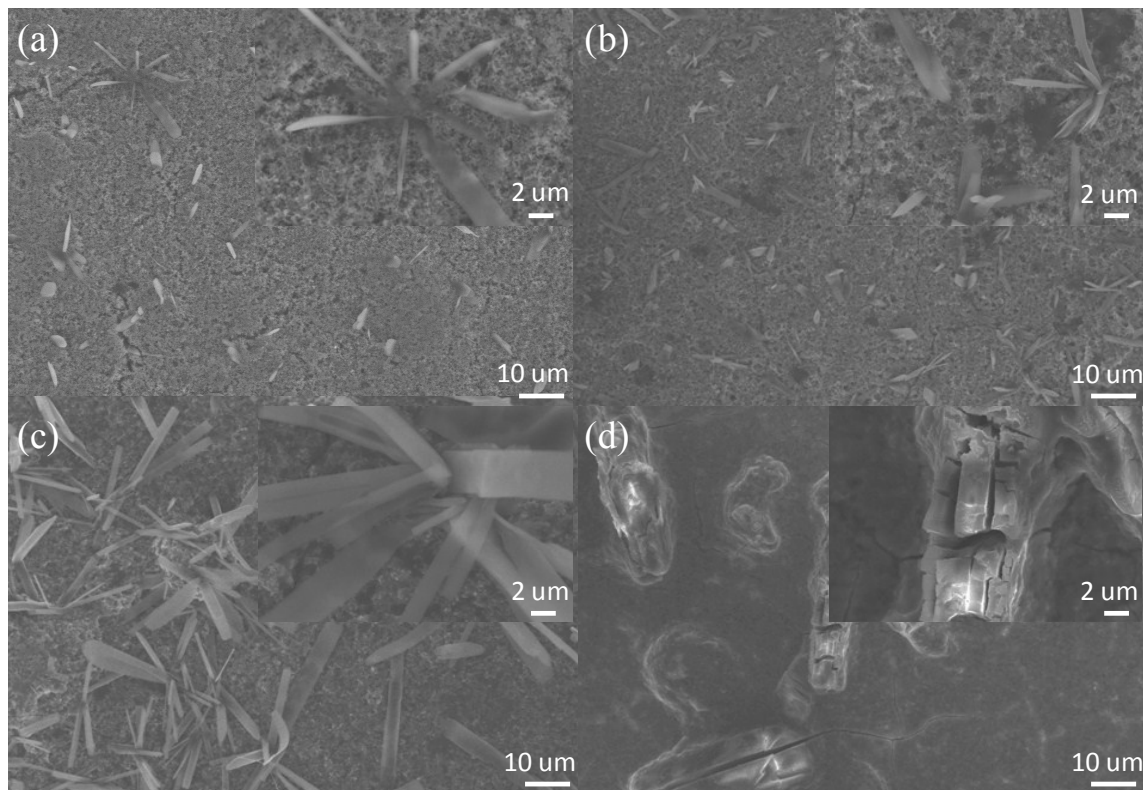
Figure S9 SEM images of pristine IA electrodes with different IA:AB:CMC-SBR weight ratios: (a) 5:4:1 wt%, (b) 6:3:1 wt%, (c) 7:2:1 wt% and (d) 8:1:1 wt%.
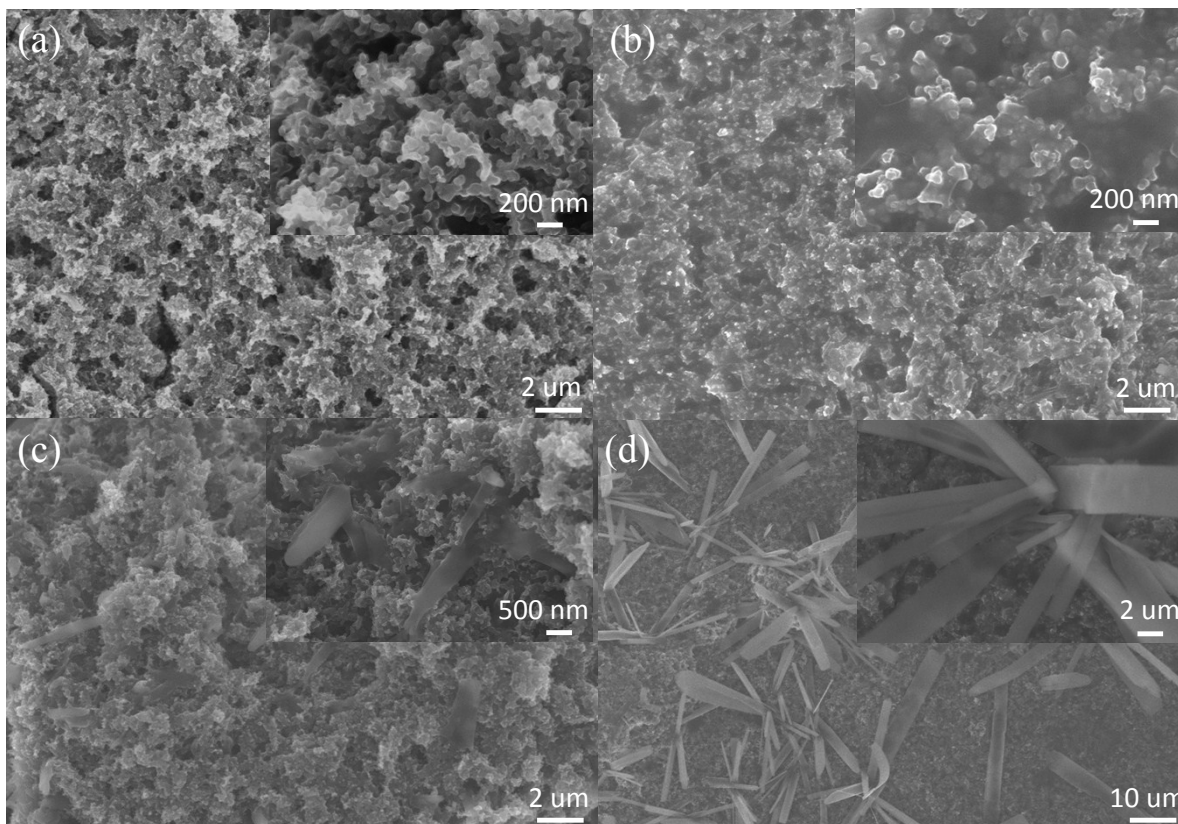
Figure S10 SEM images of pristine IA electrodes with different chemical compositions: (a) IA:AB=7:2 wt%, (b) IA:AB:CMC=7:2:1 wt%, (c) IA:AB:SBR=7:2:1 wt% and (d) IA:AB:CMC-SBR=7:2:1 wt%.

Figure S11 compared the morphologies of IA anodes (IA:AB:binder=5:4:1 wt%) with CMC-SBR, PVA and PVDF as binder, respectively. All these three electrodes have different morphology. Specifically, CMC-SBR based anode exhibits a leek-like morphology composed of ultrathin micro-ribbon (Figure S11a and b); PVA based anode shows irregular blocks agglomerated by ultrathin micro-ribbon (Figure S11c and d); while for PVDF based anode, IA distributed among AB particles in an irregular shape, and appears some strips with a diameter of 40-60 nm (Figure S11e and f). These results indicate that the electrode morphology of IA anodes is related to the dissolution and precipitation process of the IA in the different binder solution.
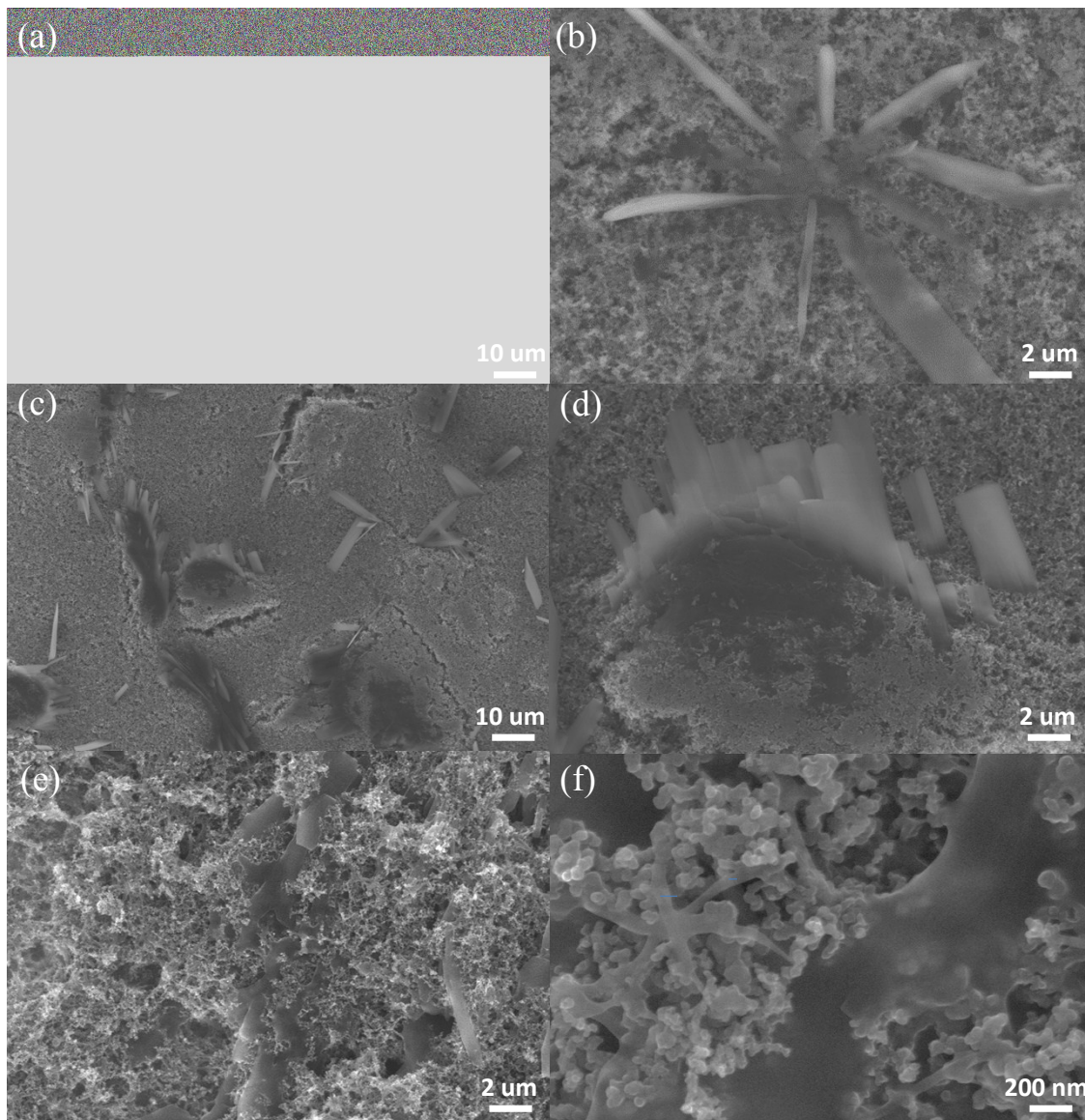
Figure S11 SEM images of the IA anode (IA:AB:binder=5:4:1 wt%) with (a and b) CMC-SBR, (c and d) PVA and PVDF (e and f) as binder.

Figure S12 compares the electrochemical performances of IA anodes (IA:AB:binder=5:4:1 wt%) with CMC-SBR, PVA and PVDF as binder, respectively. The first reversible specific capacity of CMC-SBR, PVA and PVDF based IA anode is 1270, 660 and 508 mAh g^{-1}, respectively; the corresponding first coulombic efficiency is 66.2, 51.4 and 47.6, respectively

(see Figure S12a). The lower capacity of PVA and PVDF based anodes is because of the severe agglomeration in the electrodes (see Figure S11c-f). The specific capacity at various current densities is CMC-SBR>PVA>PVDF based anode (see Figure S12b). These results indicate that the electrode morphology plays an important role in the electrochemical performance of IA anodes. And the leek-like structure resulted from the synergistic effect between IA, SBR and CMC exhibits the highest electrochemical performances.
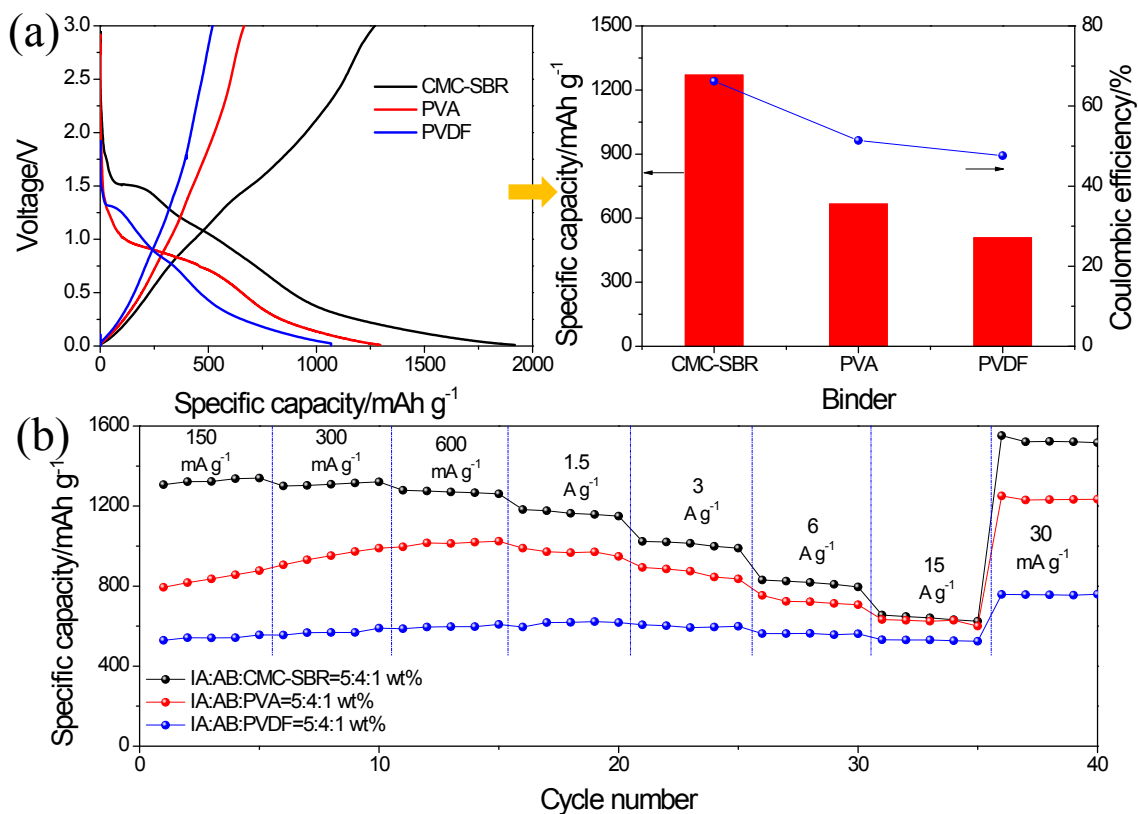

Figure S12 (a) The first charge/discharge curves of IA anodes (IA:AB:binder=5:4:1 wt%) with different binder at 30 mA g^{-1} and the corresponding capacity and the coulombic efficiency, and (b) the rate capability at various current densities after five formation cycles.
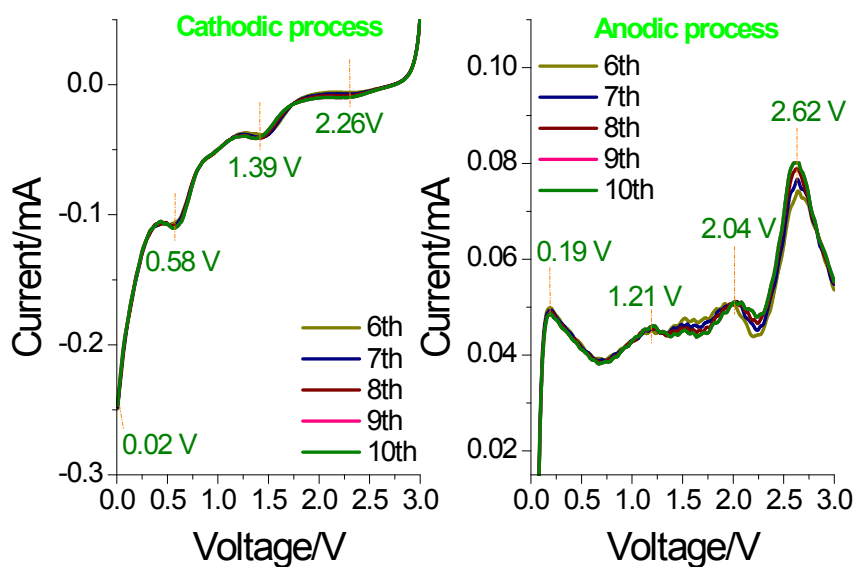
Figure S13 The separated cathodic and anodic process of the CV curves from six to ten cycles of the IA electrode in the voltage range of 0.01-3.0 V
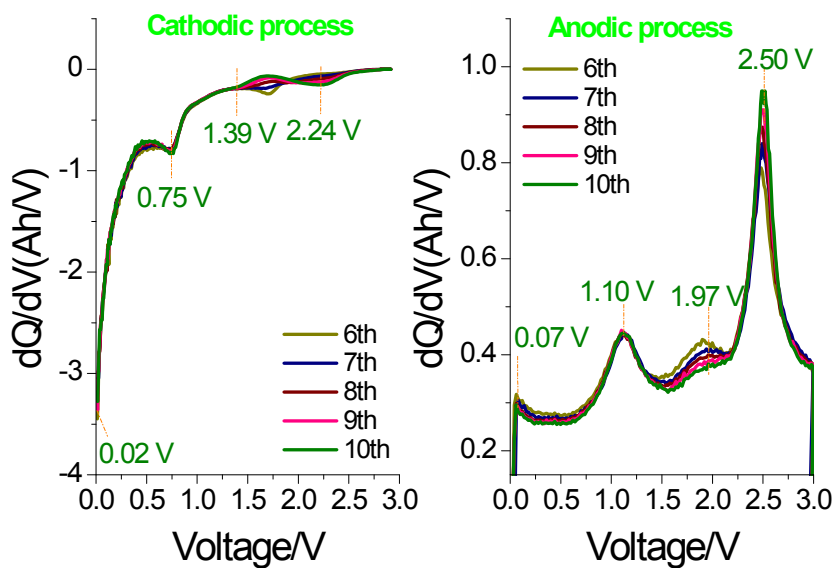

Figure S14 The separated cathodic and anodic process of the differential capacity plots (dQ/dV versus cell potential) from six to ten cycles of the IA electrode in the voltage range of 0.01-3.0 V.

To investigate the effects of cycle number on the IA structure, *ex-situ* XPS measurements for the samples retrieved from the dismantled cells at fully delithiated state after different electrochemical cycles (Figure S15a) were conducted. Figure S15b shows the collected Li1s spectra of the IA anode after different electrochemical cycles. For all the samples, the typical Li1s signal reflects that some lithium ions are not extracted from the IA electrode due to the strong irreversible reactions in the first cycle. As seen in Figure 15c and d, both the C1s and O1s spectra of the IA anode retain stable after four cycles, manifesting the IA electrode underwent an activation process in the initial several cycles.
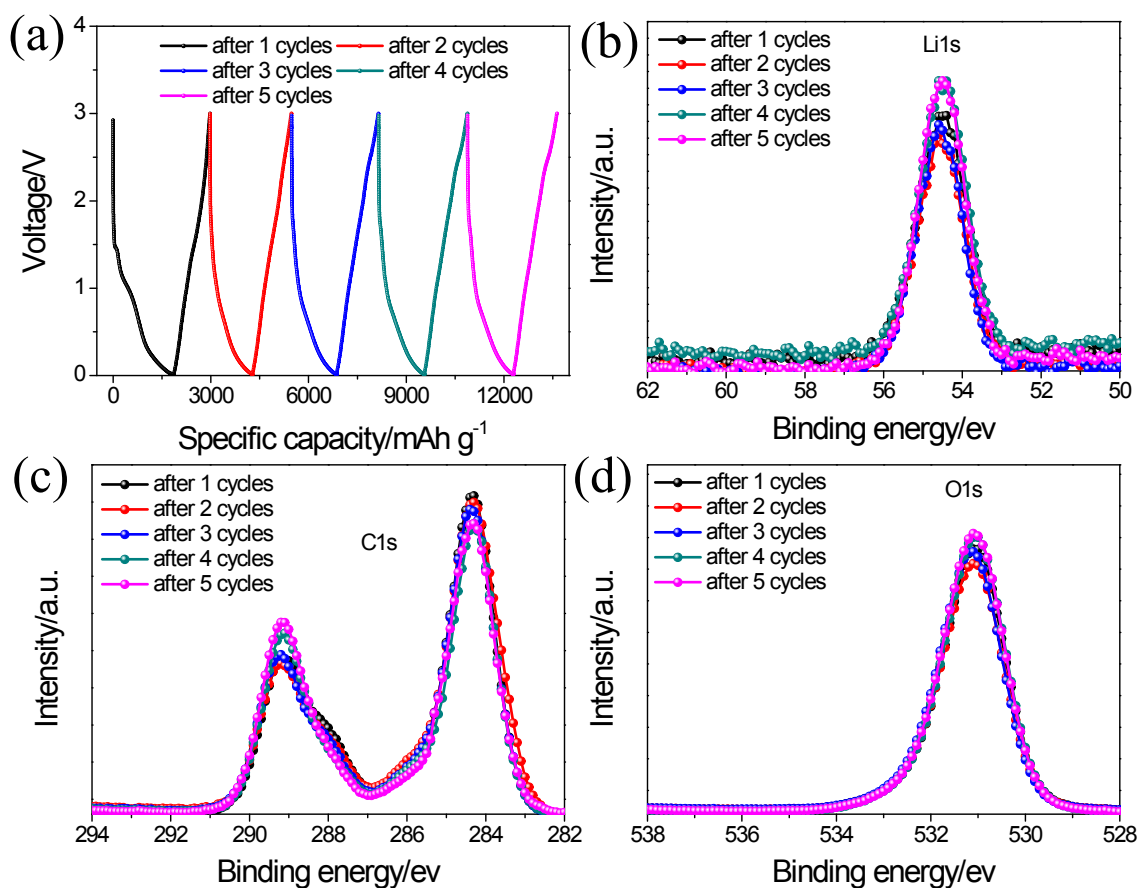

Figure S15 (a) IA electrodes selected for XPS measurements after different cycles. XPS spectra of (b) Li 1s, (c) C 1s, and (d) O 1s of IA electrodes after different cycles.